

Cover Page



Universiteit Leiden



The handle <http://hdl.handle.net/1887/37612> holds various files of this Leiden University dissertation

**Author:** Marel, Kim van der

**Title:** Unraveling the implanted cochlea : radiological evaluation of cochlear morphology and electrode position in CI patients

**Issue Date:** 2016-02-10

## Chapter Four



# Diversity in Cochlear Morphology and its Influence on CI Electrode Position

*Publication Ear and Hearing (2014)*

Kim S. van der Marel MD, Jeroen J. Briaire PhD, Ron Wolterbeek MD,  
Jorien Snel-Bongers MD, Berit M. Verbist MD PhD and Johan H.M. Frijns MD PhD

## ABSTRACT

### Objectives

To define a minimal set of descriptive parameters for cochlear morphology and study its influence on the cochlear implant electrode position in relation to surgical insertion distance.

### Design

Cochlear morphology and electrode position were analyzed using multiplanar reconstructions of the pre- and postoperative CT scans in a population of 336 patients (including 26 bilaterally implanted ones) with a CII HiFocus1 or HiRes90K HiFocus1J implant. Variations in cochlear diameter and cochlear canal size were analyzed. The relationship between the outer and inner walls was investigated. Size differences based on sex, age, and ear side were investigated using linear mixed models. Two new methods, spiral fitting and principal component analysis, were proposed to describe cochlear shape, and the goodness of fit was investigated. The relationship between cochlear shape and electrode position, in terms of modiolus proximity and insertion depth, was analyzed using clustering, one-way analysis of variance (ANOVA) and simple linear regression analysis.

### Results

Large variations in cochlear morphology were found, with cochlear canal sizes ranging from 0.98 to 2.96 mm and average cochlear diameters between 8.85 and 5.92 mm (with standard deviations of around 0.4 mm). The outer and inner walls were significantly correlated ( $p < 0.01$ ), and a size difference of 4% in favor of males was found. Spiral fitting shows good alignment of the true measurements, with residuals having a mean of 0.01 mm and a standard deviation of 0.29 mm.

Principal component analysis (PCA) showed that the use of one component, which describes size, is sufficient to explain 93.6% of the cochlear shape variance. A significant sex difference was also found with spiral fitting and PCA. Cochlear size was found to have a significant influence on modiolus proximity and insertion depth of the electrode ( $p < 0.01$ ). Cochlear size explained around 13% of the variance in electrode position. When cochlear size was combined with surgical insertion, more than 81% of the variance in insertion depth can be explained.

### Conclusions

This study demonstrates a large variety in cochlear morphology, which significantly impacts electrode position in terms of modiolus proximity and insertion depth. The effect size is, however, relatively small compared with surgical insertion distance. PCA is shown to be an accurate reduction method for describing cochlear shape.

## INTRODUCTION

Cochlear Implantation is a well-established therapy for patients with severe to profound hearing loss. Among patients, however, a wide variability in performance is observed. Electrode positioning has been indicated to be one of the factors that influence cochlear implant (CI) performance, and adjusting this may further improve the hearing scores of implantees (Aschendorff et al. 2007; Finley et al. 2008). Three factors that influence electrode position can be identified; cochlear anatomy, surgical insertion, and electrode design. Intracochlear trauma and loss of residual hearing are some of the unfortunate outcomes that can sometimes be prevented by controlled surgical insertion and the use of a patient-appropriate electrode design (Adunka & Kiefer 2006; Aschendorff et al. 2007). Other than its design and surgical insertion, the position of the electrode is also influenced by the morphology of the cochlea (Dimopoulos & Muren 1990; Ketten et al. 1998; Escude et al. 2006). This study investigates a minimal set of descriptive parameters for the human cochlear morphology and its influence on the electrode position in combination with the variability due to surgical insertion distance. Descriptive parameters will facilitate the development of a future predictive model for insertion depth to guide the surgeon during insertion, hopefully thereby creating conditions that help to maximize performance.

Cochlear morphology has been studied by several groups, both radiologically and histologically. The radiological analysis by Escudé et al. (2006) shows a wide spread of about 2.0 mm (95% CI) in overall size of the basal turn of the cochlea. This is in line with the described variations (from 7.08 mm to 9.16 mm) in cochlear basal diameter among the 20 patients studied by Ketten et al. (1998). They also measured cochlear length and found it to range between 29.07 and 37.45 mm. The histological analysis performed by Erixon et al. (2009) showed similar variations in cochlear morphology, including spiral length, and the authors also stated that each cochlea has its own “fingerprint,” an individual design with variable proportions.

Defining the exact cochlear shape with a limited set of parameters remains a challenge. In mathematical studies, cochlear shape has been approximated by different spiral functions, mostly based on either the Archimedean or logarithmic spiral (Ketten et al. 1998; Yoo et al. 2000). These methods result in accurate descriptions, but require elaborate postprocessing procedures. Thus, an easily applicable method for defining cochlear shape is needed for clinical purposes, but is not yet available. Moreover, it is necessary to investigate whether



direct size measurements, like cochlear diameters, are sufficient to describe the influence on insertion depth. The primary goal of this study was to identify one or two variables by which cochlear morphology can be best described.

Besides cochlear morphology, surgical insertion technique and electrode design are two other known factors that influence electrode position. Unlike the morphology of the cochlea, which is patient specific and fixed, surgical insertion technique and choice of electrode design are adjustable factors. Various surgical techniques and electrode designs have been developed to facilitate atraumatic or controlled positioning of the electrode (Gstoettner et al. 1997; Tykocinski et al. 2000; Eshraghi et al. 2003; Aschendorff et al. 2007; Rebscher et al. 2008; Verbist et al. 2009; Ibrahim et al. 2011; Iverson et al. 2011; Kahrs et al. 2011). The electrode can be inserted using a round-window approach or via a cochleostomy, with both methods showing comparable outcomes in terms of insertion trauma and residual hearing preservation (Adunka & Kiefer 2006; Skarzynski et al. 2007). Alternatively, the crista ante fenestram can be drilled away, defined as an extended round-window approach, reducing the chances of preserving residual hearing. Analyzing the influence of insertion variations and cochlear morphology on electrode positioning will allow surgeons more control over surgical results (Finley et al. 2008). Moreover, it provides feedback to the surgeon, which might improve surgical skills (Finley et al. 2008).

With regard to electrode design, acquiring more knowledge about cochlear morphology can also be of great value for the surgeon in selecting the patient-appropriate electrode and for development of future implant designs. Escudé et al. (2006) showed a large impact of cochlear size variations on both linear and angular insertion depth for straight and perimodiolar electrode types. Research could either focus on an electrode type that fits most cochleas or develop a tailor-made electrode for each individual patient. The FLEX electrode series of Med-El (Medical Electronics, MedEl, Innsbruck Austria) are an example of such tailor-made electrode types (MED-EL, 2012). Although these electrodes are clinically available for cochlear implantation, few CI centers use individualized, preoperative electrode selection for a standard cochlear implantation. A secondary goal of this study was to determine the degree to which electrode position is influenced by cochlear morphology, and to what extent the final position can be influenced by the surgeon.

To reach these two goals, we searched for a clinically applicable method for defining the shape of an individual cochlea. This method must be available for surgeons during the process of preoperative electrode selection, and consist of only a few variables that can be obtained



from clinical images. Several directly measured and some derived variables, based on fitting formulas and reductional statistical analysis, were studied. These derived variables had the advantage of being less correlated to each other than directly measured variables. The correspondence of the derived variables with the directly measured variables was tested. Also, differences in cochlear morphology and its variations (sex, age and ear side) among subgroups were investigated. Finally, the relationship between cochlear shape and final electrode position was illustrated, while controlling for variations in surgical insertion distance.

## PATIENTS AND METHODS

### Patients

For this study data of 401 patients who sequentially received a CII implant with HiFocus1 electrode or a HiRes90K with HiFocus1J electrode manufactured by Advanced Bionics (Advanced Bionics, Sylmar, CA) between September 2002 and December 2011 at Leiden University Medical Center, The Netherlands, was collected (all without a positioner). The study was restricted to this lateral wall electrode type because of the visibility of the individual contacts on postoperative CT scans. Five cases with abnormal insertion, 26 cases with abnormal cochlear morphology, and 34 cases with poor-quality scans (all obtained during first years of implantation, when the CI scanning protocol was still being fine-tuned) were excluded. In the end, the population consisted of 336 patients, including 26 bilaterally implanted patients, thus 362 implanted cochleas. The CT scans of 671 cochleas were analyzed (for 1 patient there was no scan obtained of the nonimplanted cochlea). Demographic details of the included population are shown in Table I. In all these patients surgery resulted in complete and uncomplicated insertions, using an extended round-window approach.

### Image Reconstruction and Analysis

As part of the standard workup for cochlear implantation at our center, all patients are scanned before and 1 day after surgery with a CT scanner (scanner type: Aquilion 4, Aquilion 16, Aquilion 64, Aquilion 1; Toshiba Medical Systems, Otowara, Japan) and multiplanar reconstructions (MPRs, voxel size:  $0.015 \text{ mm}^3$ ) were made from these scans (Verbist et al. 2005, 2010a). To study cochlear sizes and their relationship to insertion depth, the MPRs of each patient were analyzed by applying a three-dimensional coordinate system



(Verbist et al. 2010b). This coordinate system enables surgeons and researchers to assess individual MPRs and measure cochlear sizes and electrode positioning without the use of a universal template (Verbist et al., 2010a, 2010b).

To analyze cochlear size, the outer and inner wall distances to the center of the modiolus were defined by scrolling through the preoperative MPR slices in the plane of the basal turn of the cochlea using an in-house designed postprocessing program (Matlab, Mathworks, Novi, MI; Figure 1A).

**Table 1.** Demographic details of studied patients (N=336)

Gender	N	%
Male	153	46
Female	183	54
Age at implantation (yrs)	N	%
Age ≤ 2 yrs	51 <sup>1</sup>	15
Age > 2 yrs	285 <sup>1</sup>	85
	Mean	SD
Age at onset of HL (yrs)	13	19
Duration of deafness (yrs)	20	19
Age at implantation (yrs)	41	26
Etiology	N	%
Congenital	168	50
Hereditary	93	
Acquired	30	
Unknown	45	
Acquired	95	28
Meniere's disease	6	
Infectious	50	
Otosclerosis	6	
Ototoxicity	12	
Trauma	8	
Unknown	13	
Unknown	73	22

<sup>1</sup> One child was sequentially implanted and received a second implant at the age of 9 years.



As these distances are measured along four axes, this results in four diameters (=8 radii) and eight cochlear canal sizes for the basal turn of the cochlea. Two of these axes are in accordance with the consensus on cochlear coordinates (Verbist et al. 2010b) and conform to the cross-sections used by Escudé et al. (2006), consisting of a line connecting the center of the round window to the center of the modiolus (radius 1 and 5) in combination with a perpendicular line (radius 3 and 7) lying within the plane of the cochlear basal turn. The other two axes derive from the Leiden coordinate system, as described by Verbist et al. (2005), and are defined by a line connecting the center of the modiolus to the most lateral point of the horizontal semicircular canal (radius 4 and 8) combined with a perpendicular line (radius 2 and 6), again in the abovementioned plane. This system is especially useful for the assessment of postoperative MPRs, as the horizontal semicircular canal remains stable (it can be difficult to identify the center of the round window postoperatively after using a [extended] round window approach). The average rotational angle between the consensus coordinate system and the Leiden coordinate system for the studied population was 33 degrees with a standard deviation of 3.51 degrees. The accuracy of this method was evaluated in a previous study showing good intraclass correlation coefficients (ICCs) and small standard deviations for both angular (ICC 0.74-1; SD<5 degrees) and linear measurements (ICC 0.77-1; SD<0.5mm) within the cochlea (Verbist et al. 2010a).

Postoperative MPRs were assessed to visualize several electrode position measurements (Figure 1B). Every indicated position was expressed in an “angular” (degrees from the round window) and “linear” (millimeters between two positions) manner. For each of the 16 electrode contacts the distance from the contact center to the inner wall of the cochlea and center of the modiolus was measured. The position of the most apical contact (electrode contact 1:E1) defined the angular insertion depth. The distance from the round-window center (RW) to the most basal contact (electrode contact 16:E16) can be mostly controlled by the surgeon and is therefore designated by “surgical insertion.” To obtain this distance, the spiral length from RW to E16 was calculated using Eq. (1):

$$S(\theta) = (a \cdot \sqrt{1 + b^2} \cdot e^{b\theta(E16)} - 1) / b \text{ with } a=r(RW) \text{ (r is radial distance to center of modiolus)}$$

$$\text{and } b = \ln \frac{r(E16)}{r(RW)} \cdot \frac{1}{\theta(E16)} .$$

The formerly often used linear insertion depth is the sum of the surgical insertion distance and the standard configuration length of the electrode type (17 mm).



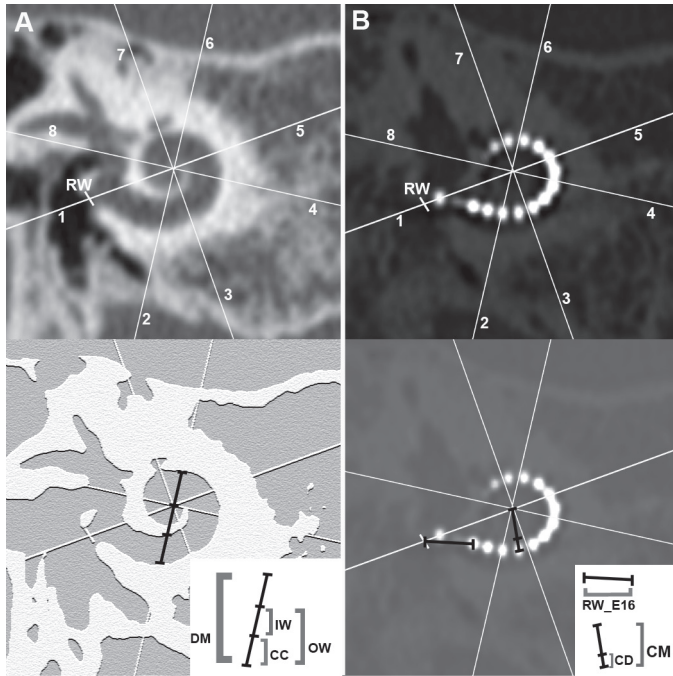


**Figure 1.** Measurements in preoperative reconstructions (A) and postoperative reconstructions (B). Upper level: True reconstructions with eight radii and round window (RW). Lower level: Schematic illustrations and measurements. The case used to explain the measurements, had an angular insertion depth of 360 degrees. Measurements on reconstruction A: DM=diameter, IW=distance inner wall-center modiolus, CC=cochlear canal, OW=outer wall-center modiolus. Diameter 1= OW radius 1+5, Diameter 2= OW radius 2+6, Diameter 3= OW radius 3+7, Diameter 4= OW radius 4+8. Measurements on reconstruction B: RW\_E16=surgical insertion, CD=contact distance to modiolar wall, CM=contact distance to center of modiolus. Consensus coordinate system: (radii 1 and 5) x (radii 3 and 7). Leiden coordinate system: (radii 4 and 8) x (radii 2 and 6)



## Derived Variables

### Clustering

To facilitate further statistical analyses, we classified some of the previously described measurements into a few, predefined number of clusters (See Appendix A Cluster Outcomes; final cluster centers and ANOVA tables). The K-sample clustering procedure in SPSS (SPSS 17.0 for Windows; SPSS Inc., Chicago, IL) attempts to identify relatively homogeneous groups of cases based on selected characteristics using a predefined algorithm. Using this procedure, a cochlear size group was obtained consisting of three clusters (small, medium, large) based on the four cochlear diameters. Clustering was also used to form a three-cluster (shallow, average, deep) surgical insertion distance group. Finally, two electrode position clusters (medial, lateral) were formed based on the 16 contact distances to the modiolar wall measured on the postoperative MPRs. The number and percentages of patients assigned to each cluster are presented in Table II and used for analysis of the relationship between cochlear size and electrode position.

### Statistical Analysis

The cochlear morphology measurements were analyzed using SPSS with  $p$  values less than or equal to 0.05 considered significant. Simple descriptive statistics were used to analyze overall cochlear canal size and diameters.

Size differences based on ear side, age (cutoff 2 years) and sex were analyzed with linear mixed models. This method inherently adjusts for correlations of measurements derived from the two cochleas of a patient, or within the same cochlea. In accordance with the work of Escudé et al (2006), it was also tested whether there was a difference in ratio of diameter 1 divided by diameter 3. The relationship between cochlear morphology and electrode position was analyzed using one-way ANOVA and multiple linear regression analyses.

Table II. Cluster measurements

Cochlear size	N	%
small	117	33
medium	171	47
large	74	20
Surgical insertion	N	%
shallow	46	13
average	162	45
deep	154	43
Electrode position	N	%
Medial	211	58
Lateral	151	42



## Methods of Describing Cochlear Shape

### *Spiral Fitting*

Modeling of the human cochlea is most often done by fitting either a logarithmic or Archimedean spiral to the cochlea in question (Skinner et al. 1994; Ketten et al. 1998; Yoo et al. 2000). For this study, in accordance with the work by Yoo et al. (2000), we chose the logarithmic spiral as it represents a more generalized function in comparison to the Archimedean spiral which is a first-order approximation of a logarithmic spiral. A logarithmic spiral is described by Eq. (2):  $r(\theta) = ae^{b\theta}$ , where  $r$  represents the radial distance to the center of the modiolus,  $\theta$  the corresponding angle and  $a$  and  $b$  coefficients. Coefficient  $a$  is proportional to cochlear size, while coefficient  $b$  defines cochlear curvature by quantifying the exponential decline in size of the cochlea with increasing angles. The spiral coefficients  $a$  and  $b$  were determined by fitting the distances to the modiolus center measured along four axes (8 radii) in the basal turn of the cochlea to an exponential function using logarithmic transformation and regression analysis. Spiral fits were determined for both the outer- and inner-wall radial distances. The goodness of fit of this method was investigated.

### *Principal Component Analysis*

Variation in the shape of the basal turn of each cochlea was also described using principal component analysis (PCA). This method derives a number of mutually orthogonal (uncorrelated) base forms from the set of measurements. For this study, cochlear morphology is analyzed as two separate sets of eight sizes (8 outer- and 8 inner-wall distances to the center of modiolus). An individual cochlea is modeled as a weighted sum of these base forms in relation to the average cochlear shape. When using the complete set of base forms, the cochlear shape can be reshaped identically from its origin. This method was optimized by minimizing the number of base forms while still accounting for 90% of the variation in individual cochlear shape, then testing the resulting goodness of fit.

## Relation between Cochlear Size and Electrode Position

The relationship between the cochlear size and electrode position is analyzed in terms of distance to modiolus and insertion depth. To investigate the relationship between cochlear size and distance to modiolus, the distribution of electrode positioning groups in the three cochlear size clusters was tested with a Chi-square test.



To illustrate and analyze the influence of cochlear size on insertion depth, again a post hoc test for trend using one-way ANOVA was executed. The relationship between cochlear size and insertion depth is also emphasized by an “insertion graph” according to the method of Escudé et al. (2006; Figure 3). This was executed by calculating the average insertion depth for each of the three cochlear size cluster groups and plotting the linear insertion depth against the angular insertion depth for all three groups. The difference in angular insertion depth between the large and small cochlear size clusters was determined at the average linear insertion depth of the whole population. This difference was tested by a multiple regression model. The relationship between insertion depth and two of the diameters, the spiral-fit coefficient and the first principal component, was tested by multiple linear regression. In addition, the influence of cochlear size on the insertion depth is presented using scatter plots with the three surgical insertion distance clusters marked by different icons and colors.

## RESULTS

### Cochlear Size

Figure 2A shows a boxplot of the outer- and inner-wall radial distances, both of which were significantly ( $p < 0.001$ ) correlated on all radii, ranging from Pearson's  $R = 0.76$  (radius 1) to  $R = 0.45$  (radius 8). Cochlear canal sizes are represented in Figure 2B as radius along each of the eight previously described radii. To quantify the tapering of the cochlea shown in Figure 2, the mean canal sizes decreased from 2.96 (0 degree) to 0.98 mm (327 degrees), and for every radii the mean canal size differed significantly from the mean canal size of adjacent radii ( $p < 0.003$ ), except for radii 7 and 8 ( $p = 0.95$ ). The mean cochlear canal size declines, although somewhat surprisingly, nonmonotonously, with increasing angle from 2.07 mm for radius 1 to 1.74 mm for radius 8. Table III shows the preoperative imaging characteristics. The mean cochlear diameter declined from 8.85 to 5.92 mm with standard deviations between 0.37 and 0.45 mm. The mean cochlear diameters were significantly different ( $p < 0.001$ ) between males and females, ranging from a 3.0 to 4.4% larger diameter on average in males. The ratio mean diameter of radius 1 to mean diameter of radius 3 was 1.35 and was not significantly different between males and females ( $p = 0.23$ ). Linear mixed model analyses of cochlear size as related to ear side and age showed no significant size differences ( $p = 0.18$ ;  $p = 0.21$ ). However, the effect of sex on cochlear size is significant ( $p < 0.001$ ), with male cochlea being on average 4% larger.



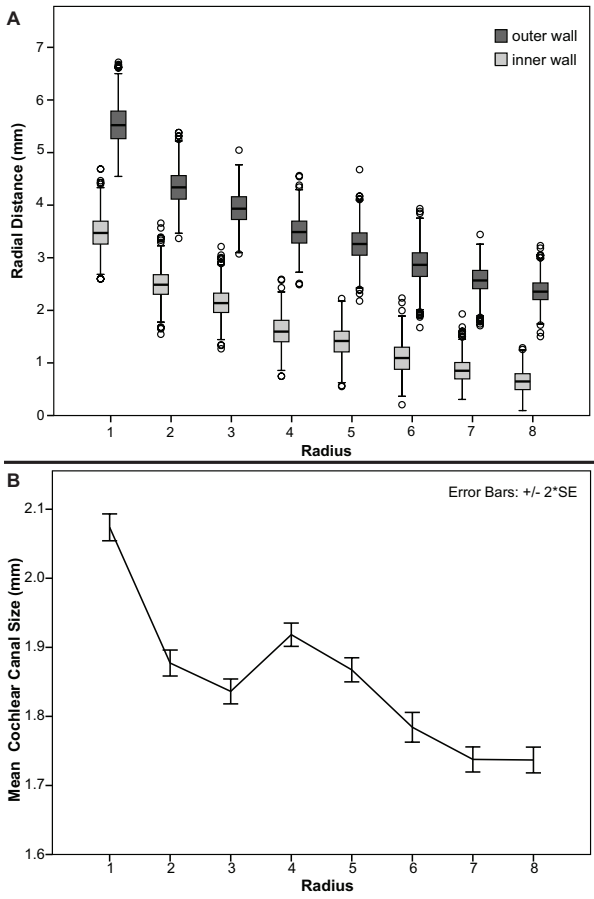


Figure 2. A: Outer and inner wall radial distances. B: Mean cochlear canal sizes for each radius and error bars representing  $2 \cdot SE$  ( $n=671$ ).



**Table III.** Imaging measurements (N=671)

Cochlear diameter (mm)	Mean (SD)
Diameter 1 <sup>1</sup>	8.85 (0.45)
Diameter 2	7.26 (0.45)
Diameter 3 <sup>1</sup>	6.58 (0.40)
Diameter 4	5.92 (0.37)

<sup>1</sup> Diameters 1 and 3 are the same as those used by Escudé et al. (2006), where they are referred to as 'distance A' and 'distance B'.

## Describing the Cochlear Shape

### *Spiral Fitting*

Using logarithmic transformation and regression analysis, fitting formula coefficients were determined for the basal turn of each implanted cochlea. These coefficients were based on the preoperative outer- and inner-wall measurements. The spiral fitting resulted in two coefficients,  $a_{\text{outer}}$  and  $b_{\text{outer}}$ , with average values of 5.19 mm (SD = 0.33, range 4.38; 6.10) and  $-0.0025 \text{ rad}^{-1}$  (SD = 0.00036, range  $-0.0038$ ;  $-0.0015$ ), respectively. The inner wall was described by two coefficients,  $a_{\text{inner}}$  and  $b_{\text{inner}}$ , with average values of 3.19 mm (SD = 0.48; range 2.86; 5.74) and  $-0.0052 \text{ rad}^{-1}$  (SD = 0.001; range  $-0.0090$ ;  $-0.0026$ ), respectively. Figure 3A shows typical examples of true and spiral-fitted cochleas. The goodness of fit of this method is shown in Figure 3B using a histogram of outer wall residuals, which reveals a normal residual distribution with a mean of 0.01 mm and a standard deviation of 0.29 mm. The mean of the inner wall residuals was  $-0.23$  mm with a standard deviation of 0.41 mm. The spread is wider at the basis (radii 1-3) than in the middle (radii 4-8), with outer-wall standard deviations of 0.37 to 0.20 and inner-wall standard deviations declining from 0.59 to 0.20. These larger deviations can also be observed in the fitted cochlear shape examples of Figure 3A.

Each of the four coefficients ( $a_{\text{outer}}$ ,  $b_{\text{outer}}$ ,  $a_{\text{inner}}$ ,  $b_{\text{inner}}$ ) are correlated significantly ( $p < 0.001$ ) with the other three coefficients. The strongest correlation existed between  $a_{\text{outer}}$  and  $b_{\text{outer}}$  ( $R = 0.56$ ). Again, significant differences ( $p < 0.001$ ) in the mean of coefficient  $a_{\text{outer}}$  and  $a_{\text{inner}}$  were found between males and females. The mean values of the b coefficients were not significantly different ( $p > 0.68$ ), indicating similar curvature of both outer and inner walls between the two sexes. All four coefficients correlated significantly with the four diameters.



Coefficient  $a_{\text{outer}}$  showed the strongest correlation with all diameters, ranging from  $R=0.52$  (diameter 2) to  $R=0.62$  (diameter 1). The other coefficient defining cochlear size,  $a_{\text{inner}}$ , showed the second strongest correlation with all diameters, from  $R = 0.31$  (diameter 1) to  $R = 0.39$  (diameter 4).

### Principal Component Analysis

Figure 4A shows the shape of the first three components derived from the PCAs. All components accumulated with the individual factor scores define deviations from the central pathway along the cochlear canal (See Appendix B PCA Outcomes; description of method, component matrix, average PCA scores). As a consequence of analyzing the outer- and inner-wall distances as two times eight recordings, the first component defines cochlear size. Figure 4A shows that the first component remains almost constant for each radius, while the second and third components vary sinusoidally along the measured radii. As component one is constant, it defines general size. Component two has a minimum of  $-0.24$  at radius 6 and a maximum of  $0.24$  at radius 1, while component three reaches a minimum of  $-0.18$  at

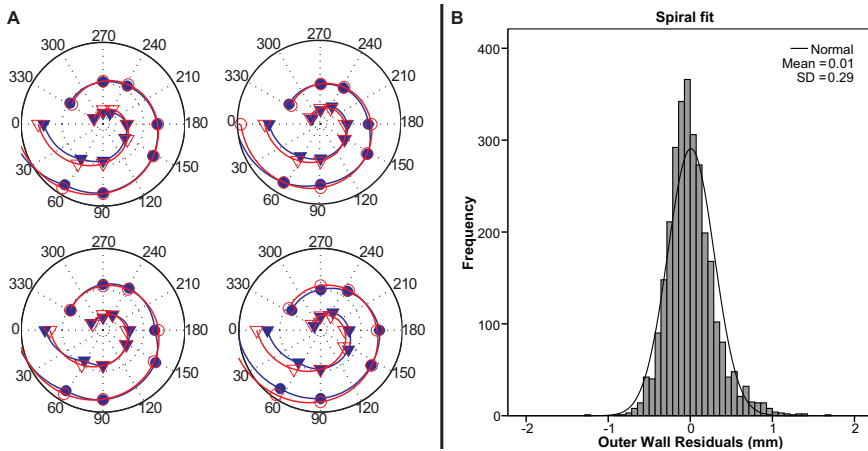


**Figure 3.** Results of spiral fitting method. A: Examples of true (blue lines) and spiral-fitted (red lines) cochlear shapes. The inner wall measurement points are marked by triangles and those of the outer wall by circles. B: Histogram of the outer wall residuals with normal distribution curve.



radius 3 and a maximum of 0.15 at radius 7. Via their sinusoidal nature, the second and third components define small broadening and narrowing adjustments at certain locations along the cochlear canal, resulting in the specific fingerprint of each cochlea. The other components define only very small changes along the eight radii. The first component explains 93.6% of the variance in cochlear shape. The second component explains only 3.0% variance and the third component less than 2.0%. On the basis of cumulative explained variance, it is evident that using one component for the outer and another for the inner measurements would sufficiently describe cochlear shape. The first component and the factor scores were used to calculate the fitted PCA outcomes for the outer- and inner-wall distances. Figure 4B shows examples of the true and PCA-fitted cochlear shapes. Figure 4C shows the goodness of fit histograms of the calculated residuals between the true and PCA-fitted outer walls using one, two and three components. The mean of the residuals was 0.02 mm. The standard deviation decreased from 0.27 mm to 0.13 mm with increasing number of components used (1 to 3 components). With component 1, the mean of the residuals between the true and PCA-fitted inner-wall distances was 0.02 mm with a standard deviation of 0.24 mm. The standard deviations did not differ among the different measurement radii.

Again, a significant difference in mean factor scores with component 1 was found for the outer and inner wall between males and females ( $p < 0.001$ ). However, no significant sex difference was found for component 2 or 3 (all:  $p > 0.09$ ). Furthermore, a strong correlation was found between component 1 and all four diameters ( $p < 0.001$ ). The correlations between component 1 of the outer walls and the diameters were between  $R = 0.85$  and  $R = 0.91$ . For the inner walls, correlations with the diameters were between  $R = 0.40$  and  $R = 0.55$ . The other components were not correlated with these diameters.

When clustering into three groups was repeated based on only component 1 and cluster numbers were compared to the original cluster group numbers based on the four diameters, high levels of correspondence were found. Of the small cochleas 90.1% were classified into a small cluster group by both forms of clustering. For the middle-sized cochleas, 94.8% correspondence between two forms of clustering was found with 99.0% correspondence for the large-sized cochleas.



## Relation between Cochlear Size and Electrode Position

### *Influence of Cochlear Size on the Distance to Modiolus*

The distribution of the medial and lateral electrode positioning groups in the three cochlear size clusters was tested with a Chi-square test and showed a significant difference in distribution between the three cochlear size cluster groups ( $p < 0.001$ ).

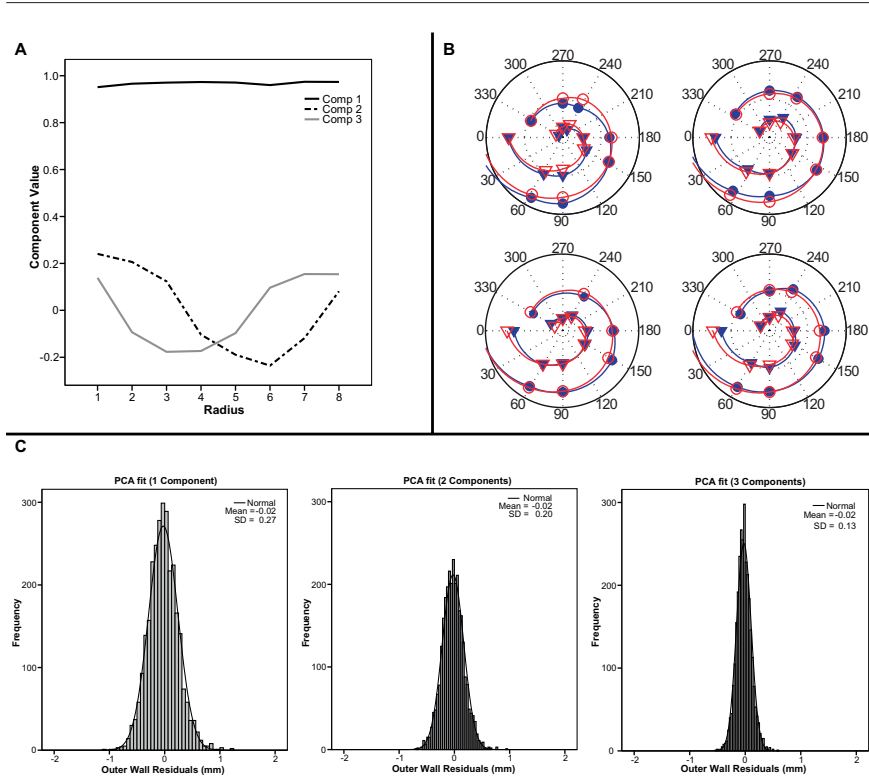


**Figure 4.** Results of PCA. **A:** Values of the first three components on all radii. **B:** Examples of true (blue lines) and PCA-fitted (red lines) cochlear shapes. The inner wall measurement points are marked by triangles and those of the outer wall by circles. **C:** Histograms of PCA-fitting residuals of the outer walls with 1, 2, and 3 components. The lines represent normal distribution curves.



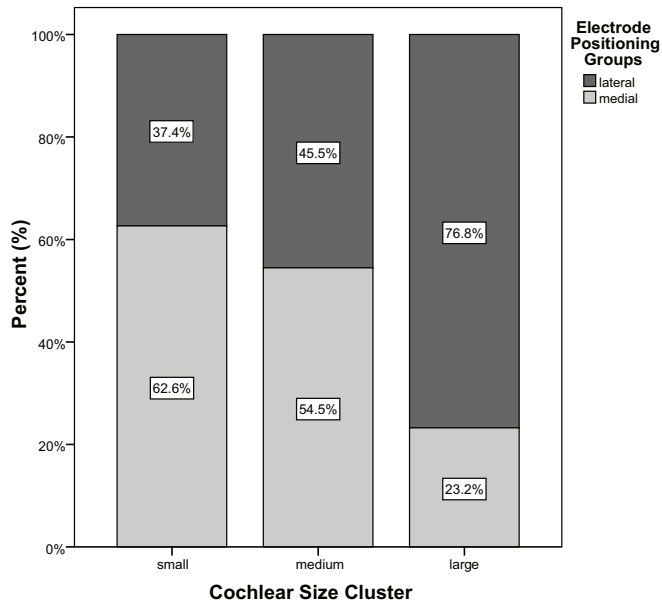


Figure 5. Distribution of electrode positioning groups in the three cochlear size clusters.

The percentages of medial and lateral electrode positioning groups in the small, medium, and large cochleas are shown in Figure 5, illustrating the different distribution among the groups.

#### *Influence of Cochlear Size on the Final Insertion Depth*

In addition, the relationships between the cochlear size and shape and their influence on the insertion depth were analyzed. The mean (angular) insertion depth was 480 degrees and the mean surgical insertion distance (distance from round window to most basal contact) was 6.53 mm. All diameters were negatively correlated with insertion depth. For all diameters, the Pearson's correlation coefficients with insertion depth were  $R = -0.3$  ( $p < 0.001$ ). Figure 6 shows the insertion depth for each of the three cochlear size groups. The significance of the relationship between cochlear size and insertion depth was supported by a test for trend using a one-way ANOVA ( $p < 0.001$ ).



This relationship is further illustrated by Figure 7, where the linear insertion depth of the most apical electrode contact (E1) is plotted against the angular insertion depth. The different cochlear size clusters are denoted using regression lines and varying symbols. The average value for diameter 1, titled “distance A” by Escudé et al. (2006), was 8.5 mm for small cochleas and 9.4 mm for large cochleas, respectively. For the studied population, the average surgical insertion distance was 6.53 mm and the average linear insertion depth was 23.0 mm. For this average linear insertion depth (vertical line), the average difference in insertion angle between small, medium and large cochleas is shown in the figure, resulting in a difference of 68 degrees between the small and large cochleas (horizontal lines). This difference in angular insertion depth between the small and large cochlear size clusters for all linear insertion depths was highly significant ( $p < 0.001$ ), as demonstrated using a linear regression model.

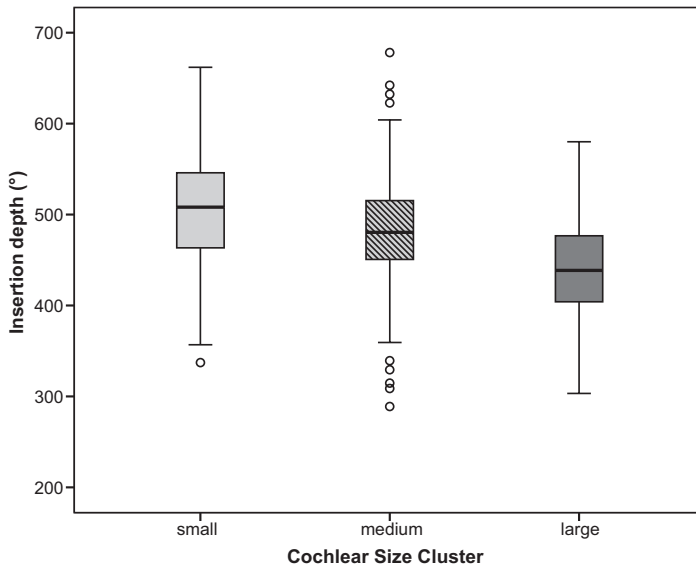


Figure 6. Angular insertion depths of the three cochlear size clusters.



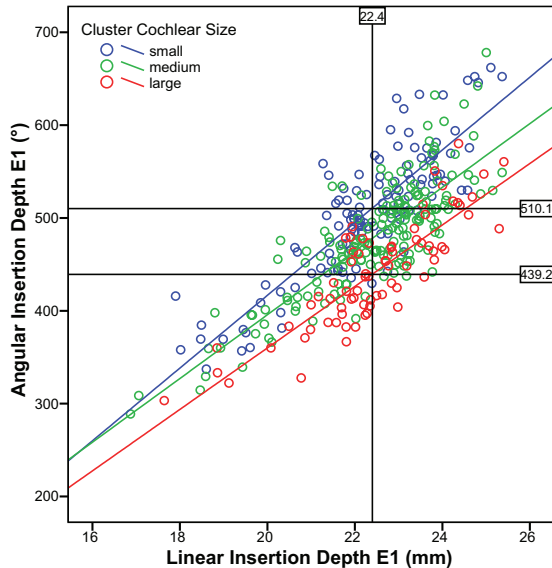


Figure 7. Linear insertion depth of the most apical E1 versus angular insertion depth E1. Vertical line shows the average linear insertion depth of 22.4 mm. The upper horizontal line shows the average insertion angle for the small cochleas group and lower horizontal line shows average angle for large cochleas.

Figure 8 shows the relationship between cochlear sizes and surgical insertion distance on insertion depth. Surgical insertion distance was clustered into the three groups (Table III) and marked with different symbols and colors in the figure. Figure 8A and B show scatterplots of the two cochlear diameters (diameter 1 and 2) versus the insertion depth. The same plots were obtained for the spiral coefficient  $a_{\text{outer}}$  in Figure 8C and the PCA component 1 in Figure 8D. When surgical insertion distance clusters are analyzed separately, downward trend lines between cochlear size and insertion depth can be observed. The slopes of the downward trend lines for the different surgical insertion distance groups differed between the two diameters (Figure 8A versus 8B). Also, downward trends can be observed when using the spiral- or PCA-fit variables (Fig 8C versus 8D).



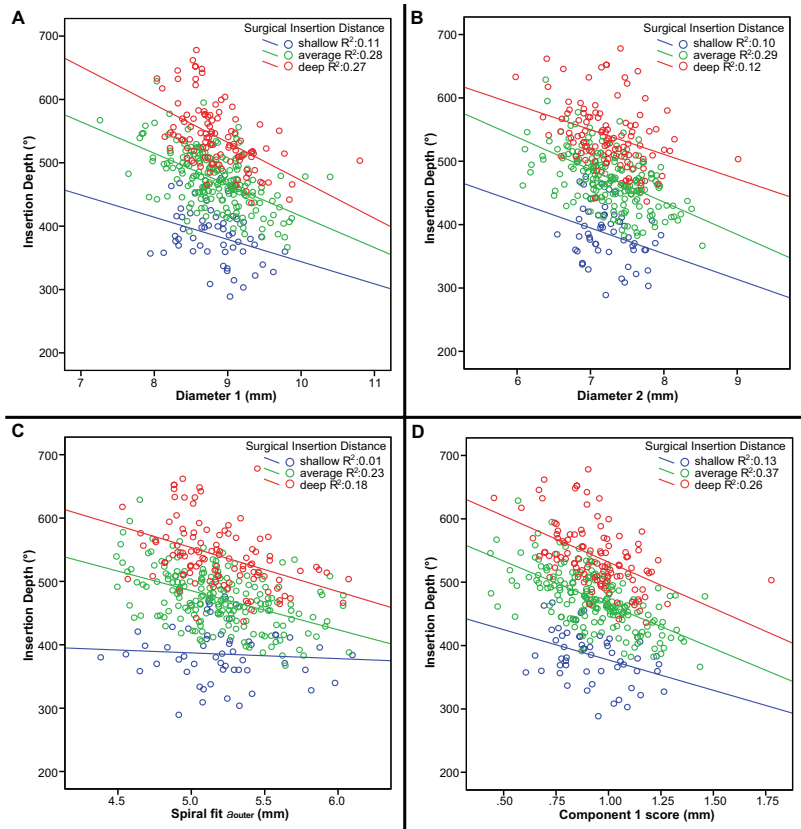


Figure 8. Relationship between the two cochlear diameters 1 (A) and 3 (B), spiral-fit coefficient  $a_{outer}$  (C), PCA component 1 (D), and insertion depth, analyzed separately, for different surgical insertion distances. The three surgical insertion distance groups are denoted using varying symbols and colors. A trend line is fitted for each surgical insertion distance group.



However, the spiral-fit trend lines are not as steep as those of the PCA-fit trend lines. In the spiral-fit plot, an almost horizontal trend line can be observed for the shallow surgical insertion distance group, indicating almost no relationship between spiral coefficient and insertion depth. The difference in insertion depth between the different surgical insertion distance clusters, when tested for the diameters 1 and 2, spiral fit  $a_{\text{outer}}$  and principal component 1 using multiple regression models, was highly significant ( $p < 0.001$ ) in all models, with a mean difference of around 150 degrees between the shallow and deep surgical insertion distance clusters.

The relationship between insertion depth and the two proposed methods for defining cochlear shape was tested by regression analyses (Table IV). This relationship was compared with the relationship between insertion depth and the four cochlear diameters. All analyses showed that cochlear size variables only accounts for a small percentage of variance in insertion depth. A regression model with the four diameters as predictors resulted in 12.1% of explained variance. In that model, only diameter 1 explained a significant part of variance ( $p = 0.024$ ), while the other diameters did not significantly add more explained variance to the model having  $p$  values of above 0.24. Using only diameter 1 resulted in 10.1% of explained variance. A model using spiral-fitting coefficients  $a_{\text{outer}}$  and  $b_{\text{outer}}$  as predictors explained 13.5% of the observed variance and both coefficients showed significant contribution to the model.

**Table IV.** Relation between insertion depth, cochlear shape and surgical insertion distance

Regression Models	Explained Variance of Insertion Depth (%)
Diameter 1	10.1 %
Diameter 1 + diameter 2 + diameter 3 + diameter 4	12.1 %
Spiral fit coefficient $a_{\text{outer}}$ + coefficient $b_{\text{outer}}$	13.5 %
PCA component 1 + component 2 + component 3	13.1 %
Surgical insertion distance	65.3 %
Surgical insertion distance + diameter 1	78.1 %
Surgical insertion distance + diameters 1 - 4	81.1 %
Surgical insertion distance + spiral fit coefficient $a_{\text{outer}}$ + coefficient $b_{\text{outer}}$	78.8 %
Surgical insertion distance + PCA components 1 - 3	80.4 %



In the model with PCA components for the outer wall, 13.1% of the variance was explained. Only component 1 shows a significant contribution to the model. The coefficients of components 2 and 3 were not significant.

Although the amount of explained variance by variables defining cochlear size was demonstrated to be low in all of the formulated models, use of the predictors of the newly proposed methods did not show a decline in the percentages of explained variance, but contributed by slightly higher percentages.

Moreover, the percentage of variance explained rose when surgical insertion distance was added to the three models. The model using four diameters explained 81.1% of variance, with the model using only the first diameter explaining 78.1%. The models with spiral-fitting predictors and PCA predictors, explained 78.8% and 80.4% of variation, respectively. Surgical insertion distance alone explained 65.3% of the variance in insertion depth.

## DISCUSSION

This study reports on the diversity in cochlear shape and the impact of cochlear shape on electrode position in a large clinical population. Analysis of CT scans of a large clinical population showed that cochlear sizes were measured along eight measurement radii, resulting in four basal turn diameters and eight cochlear canal sizes. Both diameters and canal sizes showed large variation with standard deviations of 0.4 mm along all radii. A significant sex difference was found, with males having a 4% larger cochlea on average. Spiral fitting and PCAs were shown to be able to reduce the number of variables needed to describe cochlear shape accurately. Using PCA, 93.6% of the variance in cochlear shape can be described with only one component for the outer and one for the inner walls. The size of the cochlea significantly influences electrode position in terms of modiolus proximity and insertion depth. Cochlear size alone explains around 13% of variance in insertion depth. When combined with surgical insertion distance, 75% of the variance can be explained.

Only a few previous studies have reported on anatomical variance in the normally developed cochlea. A diameter of the basal turn of the cochlea, comparable with diameter 1 in this study, was previously measured by Erixon et al. (2009). They reported a mean width of 6.8 mm (SD 0.46 mm) with a range of 5.6 to 8.2 mm. This mean diameter is slightly smaller than the 8.84 mm measured in this study. Escudé et al. (2006) measured two diameters (“A” and “B”)



which are comparable with diameters 1 and 3 of this study. The Escudé diameter A mean was 9.23 mm versus a mean diameter 1 in this study of 8.84 mm while Escudé diameter B mean was 6.99 mm (SD = 0.37) compared with 6.58 mm (SD=0.40) for diameter 3 in this study. However, the diameters found in this study were slightly larger than reported by Erixon et al. and smaller than reported by Escudé et al. Moreover, the measured diameter 1 is in line with the reported diameter range of 6.9 to 8.2 mm by Stakhovskaya et al. (2007).

In accordance with the studies by Roland et al. (1998) and Sato et al. (1991), no size differences based on age were found ( $p = 0.21$ ). The left and right cochleae were of similar size in this study ( $p = 0.18$ ), while Escudé et al. (2006) reported a significant ( $p < 0.001$ ) mean difference of 0.23 mm for diameter A. In the present (larger) study group, however, only a significant size difference based on sex was found ( $p < 0.001$ ). This size difference between males and females has been reported before by Escudé et al. (differences in diameter A  $p < 0.05$  and B  $p = 0.01$ ). Like the present study, the study by Escudé et al. found no significant sex difference in the ratio of A/B. The mean ratio of 1.32 in their study is comparable to the mean of 1.34 reported in the present study. Sato et al. found significant differences in cochlear canal length based on sex ( $p < 0.01$ ) while Ketten et al. (1998) found only a slightly longer cochlear canal length in males, which was not significantly in their study. This study analyzed only the basal turn of the cochlea, thus no comparison of cochlear canal length with the outcomes of Erixon et al. (2009) and Ketten et al. can be made. It seems reasonable, however, to assume that a larger cochlear size corresponds with a larger cochlear canal length.

In this study, multiplanar reconstructions were obtained and the  $z$  axis was determined during the process of reconstruction. As correctly mentioned by Escudé et al. (2006) and Stakhovskaya et al. (2007) before, comparison of the abovementioned measurements can be easily affected by only a slight shift in chosen angle of view. Moreover, a small rotation of the  $z$  axis in our study might also affect the measured and fitted curved cross-sectional shape of the cochlear canal, altering the measured individual shape of the cochlea.

The uniqueness of the cochlea's shape, the fingerprint as described by Erixon et al. (2009), emphasizes the need for methods that can accurately describe this shape. The Archimedean and logarithmic spiral are most often used to model the human cochlea (Skinner et al. 1994; Ketten et al. 1998; Yoo et al. 2000). The logarithmic spiral represents a more generalized function and was therefore chosen to model cochlear shape, in accordance with Yoo et al. (2000). This spiral fitting indicated good concordance with the true measurements of the basal turn and the coefficients were all correlated with the measured diameters (Figure 3).



Coefficient  $a_{\text{outer}}$  [Eq. (2)] defined size, and (like diameters 1 to 4) also differed significantly based on sex (males: 3.4% larger,  $p < 0.001$ ), while  $b_{\text{outer}}$  describing the curvature along the cochlear canal, was not significantly different between males and females ( $p = 0.84$ ).

As a second descriptive method, PCA was performed. A component matrix and eight components were extracted from the observed measurements. The extent to which various components explained cochlear shape variation was evaluated. One component was found to explain more than 93% of the variation in shape and was sufficient to describe cochlear shape (Figure 4). This component described cochlear size and was strongly correlated with all four diameters. Clustering based on this one component showed strong correspondence (>90% similar groups) with clustering based on four diameters. Again a significant difference of 3.5% in favor of males was found in mean factor scores for component 1 ( $p < 0.001$ ). Component 2 and 3, as these describe the fingerprint and not size, showed no significant difference based on sex ( $p > 0.09$ ), indicating again that the overall shape of male and female cochleae is apparently not different. Components 2 and 3 define locations of broadening and narrowing along the cochlear canal, defining the unique fingerprint of each cochlea as it was named by Erixon et al. (2009). However, these components do not explain more than 3% of variance and were not correlated with the diameters. Describing the cochlear shape using only component 1 and disregarding its unique fingerprint (quantified by components 2 and 3) nonetheless results in good alignment with the true measurements. However in this study, the cochlear shape was only approximated using measurements obtained on the level of the basal turn. Other features characterizing the fingerprint of the cochlea, such as the ascending aspect and tapering of the cochlear canal duct could not be approximated with the available measurements. This study thus confirms that the use of a general template, adjusted in size to fit each cochlea, is a viable option. However, templates like the one being used by Skinner et al. (2007) and Kawano et al. (1996) are derived from a single micro CT scan of one donor and reconstruction of eight male cochleas. An alternative would be to use the more universal component matrix based on the cochleas of 336 patients, as yielded with PCA in the present study.

Comparing spiral fitting to PCA demonstrated that both are suitable for the present purpose, which is to accurately define cochlear shape. The relevant measurements can be easily obtained from reconstructions of clinical CT scans and are reduced to a small number of variables used to describe the cochlear shape without losing much variation. While the spiral-fit variables are still correlated, the PCA components are unrelated to one another. The



four diameters, being highly correlated, are not suitable for multiple regression models as their interaction may mask the true contribution of each variable to the model. Moreover, the standard deviations of the residuals were broader at the basal radii than in the middle, while no differences in standard deviations along the radii were observed for the PCA-fitted residuals. Overall, PCA is preferable because the components are uncorrelated and fewer variables are needed to sufficiently explain a cochlear variance. When analyzing the goodness of fit, the histogram also showed slightly narrower standard deviations compared to those of the spiral fit. Moreover, if desired, one can make PCA fits as accurate as one wishes, by adding more components.

More research is needed to further improve measurements and fits. Improving the software to enable measurements beyond the first turn of the cochlea might lead to more accurate results, especially with deeper inserted electrode designs. Fitting of the outer radii 1 and 8 showed broader standard deviations of the residuals with the present coordinate system. Measuring beyond the basal turn might also lead to a better fit as extrapolation of the currently obtained spiral fits into the second turn shows increasing misalignment the further the fits are extrapolated. This is in accordance with several observations that the width of the cochlear canal does not diminish continuously from base to apex (Zrunek et al. 1980; Wysocki 1999; Erixon et al. 2009). For the basal turn of the cochlea this study also showed a non-continuous narrowing of the cochlear canal (Figure 2B). Moreover, addition of more measurement radii or even development of software, which automatically obtains measurements might lead to more detailed and accurate outcomes. The poor visibility of the inner wall of the modiolus on the clinically available CT scans beyond the first turn may become a limiting factor, when trying to extend the measurements and fits into the second turn.

This study also analyzed the influence of cochlear shape on electrode position. A significant impact was shown for both direct and derived variables. The measured diameters were all negatively correlated to insertion depth with Pearson's correlation coefficients of 0.3 ( $p < 0.001$ ). These coefficients are considerably lower than the significant correlation of 0.51 between diameter A and insertion depth angle as reported by Escudé et al. (2006) in a smaller cohort. Significant differences between the cochlear size cluster groups in both modiolus proximity and insertion depth were found ( $p < 0.001$ ) (Figs. 5 and 6). To illustrate this relationship, the average difference in insertion angle between the small and large cochlea groups was evaluated. For the studied population, differences in cochlear size resulted in a difference of 68 degrees in angular insertion depth on average (Figure 7).



To determine whether there is a need for patient-specific electrode lengths, an extra analysis was performed. The goal being to cover the physiological cochlear frequency range from 200 to 6 kHz, a variation in length of array should be available. To illustrate this, patients with an insertion depth around 400 degrees ( $>390$  degrees and  $<419$  degrees) were selected and the spread of distance from round window to most basal electrode was analyzed. All these patients had the same array with a length of 17 mm in total. To obtain an insertion depth of 400 degrees with this type of array, a variation in length of 19 to 24 mm is needed. Thus, to achieve full coverage of the cochlear canal up to a desired insertion angle, patient-specific electrode lengths would be required. The need for full coverage and the impact of electrode position on performance was not evaluated in this study. However, an average difference of 68 degrees in angular insertion depth or a range of 4 mm in electrode length could have a large impact on performance outcomes (a 3mm shift along the basilar membrane corresponds to a frequency change of 1 octave (Stakhovskaya et al. 2007; Greenwood, 1990)).

This study was performed in patients who received a HiFocus1 or HiFocus1J electrode. Because this electrode is a free-fitted lateral type, the electrode insertion depth can be largely influenced by the surgeon, while cochlear size morphology also have a direct influence. If this study would have been performed using a precurved (modiolus-hugging or mid scalar) electrode type, like the Nucleus Freedom (Cochlear Americas, Denver, CO) or the HiFocus MS of Advanced Bionics, the variability in final electrode position might be smaller. The precurved shape with additional markers to guide the insertion, limits the surgical freedom during insertion, theoretically resulting in a more stable insertion depth with more proximity to the modiolus. Moreover, the built-in electrode curvature is likely to be more important than the details of the cochlear anatomy.

The findings of the present study demonstrating the influence of cochlear shape and surgical insertion distance on electrode position are also essential for the development of insertion models that predict the linear surgical insertion depth necessary to reach a predefined insertion depth angle. These models may provide more control over electrode position to stimulate a desired tonotopic area of the cochlea. The described new methods used to define both cochlear shape and diameters will be considered input parameters in these models. In this study, cochlear size measurements alone describe around 13% of the variance in insertion depth. After adding the surgical insertion distance to the different models, around 80% of the variance can be explained. Compared to surgical insertion distance (65.3%), the variance of cochlear size has only a limited effect on the final insertion depth. Future studies will have



to be performed on the development of such insertion models.

Although the relation between performance, insertion depth and cochlear size is very interesting, not much literature is available on this topic. However, the recent study by Holden et al. (2013) showed several relations. In addition, this is also the topic of ongoing research at our center (in preparation).

This study demonstrates a substantial variety in cochlear shape and size and its impact on electrode positioning. A significant size difference of 4% in favor of males was found based on sex with no size difference based on ear side or age being found. Two new methods, spiral fitting and PCAs, were proposed to describe cochlear shape with PCA being the preferred method. Using PCA, a general component matrix, in combination with one individual component score for the outer and another for the inner, can accurately describe the shape of the cochlea. Cochlear morphology was proven in several ways to significantly influence electrode position, both in terms of modiolus proximity and insertion depth.



## REFERENCES

- 1 Finley CC, Holden TA, Holden LK et al. Role of electrode placement as a contributor to variability in cochlear implant outcomes. *Otol Neurotol* 2008;29(7):920-928.
- 2 Aschendorff A, Kromeier J, Klenzner T et al. Quality control after insertion of the nucleus contour and contour advance electrode in adults. *Ear Hear* 2007;28(2 Suppl):75S-79S.
- 3 Adunka O, Kiefer J. Impact of electrode insertion depth on intracochlear trauma. *Otolaryngol Head Neck Surg* 2006;135(3):374-382.
- 4 Escude B, James C, Deguine O et al. The size of the cochlea and predictions of insertion depth angles for cochlear implant electrodes. *Audiol Neurootol* 2006;11 Suppl 1:27-33.
- 5 Dimopoulos P, Muren C. Anatomic variations of the cochlea and relations to other temporal bone structures. *Acta Radiol* 1990;31(5):439-444.
- 6 Ketten DR, Skinner MW, Wang G et al. In vivo measures of cochlear length and insertion depth of nucleus cochlear implant electrode arrays. *Ann Otol Rhinol Laryngol Suppl* 1998;175:1-16.
- 7 Erixon E, Hogstorp H, Wadin K et al. Variational anatomy of the human cochlea: implications for cochlear implantation. *Otol Neurotol* 2009;30(1):14-22.
- 8 Yoo SK, Wang G, Rubinstein JT et al. Three-dimensional modeling and visualization of the cochlea on the Internet. *IEEE Trans Inf Technol Biomed* 2000;4(2):144-151.
- 9 Gstoettner W, Plenck H, Jr., Franz P et al. Cochlear implant deep electrode insertion: extent of insertional trauma. *Acta Otolaryngol* 1997;117(2):274-277.
- 10 Tykocinski M, Cohen LT, Pyman BC et al. Comparison of electrode position in the human cochlea using various perimodiolar electrode arrays. *Am J Otol* 2000;21(2):205-211.
- 11 Eshraghi AA, Yang NW, Balkany TJ. Comparative study of cochlear damage with three perimodiolar electrode designs. *Laryngoscope* 2003;113(3):415-419.
- 12 Rebscher SJ, Hetherington A, Bonham B et al. Considerations for design of future cochlear implant electrode arrays: electrode array stiffness, size, and depth of insertion. *J Rehabil Res Dev* 2008;45(5):731-747.
- 13 Verbist BM, Ferrarini L, Briaire JJ et al. Anatomic considerations of cochlear morphology and its implications for insertion trauma in cochlear implant surgery. *Otol Neurotol* 2009;30(4):471-477.
- 14 Ibrahim HN, Helbig S, Bossard D et al. Surgical Trauma After Sequential Insertion of Intracochlear Catheters and Electrode Arrays (a Histologic Study). *Otol Neurotol* 2011.
- 15 Iverson KC, Bhatti PT, Falcone J et al. Cochlear Implantation Using Thin-Film Array Electrodes. *Otolaryngol Head Neck Surg* 2011.
- 16 Kahrs LA, McRackan TR, Labadie RF. Intracochlear Visualization: Comparing Established and Novel Endoscopy Techniques. *Otol Neurotol* 2011.
- 17 Skarzynski H, Lorens A, Piotrowska A et al. Preservation of low frequency hearing in partial deafness cochlear implantation (PDCI) using the round window surgical approach. *Acta Otolaryngol* 2007;127(1):41-48.
- 18 MED-EL (2012). FLEX Portfolio The Softest, Most Flexible Electrode Arrays [MED-EL Web site]. 2012, December 13. Retrieved December 13, 2012 from <http://www.medel.com/data/downloads/MAESTRO/23236.pdf>.
- 19 Verbist BM, Frijns JH, Geleijns J et al. Multisection CT as a valuable tool in the postoperative assessment of cochlear implant patients. *AJNR Am J Neuroradiol* 2005;26(2):424-429.



- 20 Verbist BM, Joemai RM, Briaire JJ et al. Cochlear coordinates in regard to cochlear implantation: a clinically individually applicable 3 dimensional CT-based method. *Otol Neurotol* 2010;31(5):738-744.
- 21 Verbist BM, Skinner MW, Cohen LT et al. Consensus panel on a cochlear coordinate system applicable in histologic, physiologic, and radiologic studies of the human cochlea. *Otol Neurotol* 2010;31(5):722-730.
- 22 Skinner MW, Ketten DR, Vannier MW et al. Determination of the position of nucleus cochlear implant electrodes in the inner ear. *Am J Otol* 1994;15(5):644-651.
- 23 Stakhovskaya O, Sridhar D, Bonham BH et al. Frequency map for the human cochlear spiral ganglion: implications for cochlear implants. *J Assoc Res Otolaryngol* 2007;8(2):220-233.
- 24 Roland JT, Jr., Fishman AJ, Waltzman SB et al. Stability of the cochlear implant array in children. *Laryngoscope* 1998;108(8 Pt 1):1119-1123.
- 25 Sato H, Sando I, Takahashi H. Sexual dimorphism and development of the human cochlea. Computer 3-D measurement. *Acta Otolaryngol* 1991;111(6):1037-1040.
- 26 Skinner MW, Holden TA, Whiting BR et al. In vivo estimates of the position of advanced bionics electrode arrays in the human cochlea. *Ann Otol Rhinol Laryngol Suppl* 2007;197:2-24.
- 27 Kawano A, Seldon HL, Clark GM. Computer-aided three-dimensional reconstruction in human cochlear maps: measurement of the lengths of organ of Corti, outer wall, inner wall, and Rosenthal's canal. *Ann Otol Rhinol Laryngol* 1996;105(9):701-709.
- 28 Wysocki J. Dimensions of the human vestibular and tympanic scalae. *Hear Res* 1999;135(1-2):39-46.
- 29 Zrunek M, Lischka M, Hochmair-Desoyer I et al. Dimensions of the scala tympani in relation to the diameters of multichannel electrodes. *Arch Otorhinolaryngol* 1980;229(3-4):159-165.
- 30 Greenwood DD. A cochlear frequency-position function for several species--29 years later. *J Acoust Soc Am* 1990;87(6):2592-2605.
- 31 Holden LK, Finley CC, Firszt JB et al. Factors Affecting Open-Set Word Recognition in Adults With Cochlear Implants. *Ear Hear* 2013.



## APPENDIX A

### Cluster Outcomes

Clustering Cochlear Size based on 4 Cochlear Diameters (DM)

Final Cluster Centers			
	Cluster		
	Small	Medium	Large
Diameter 1	8.45	8.87	9.41
Diameter 2	6.81	7.33	7.79
Diameter 3	6.18	6.64	7.08
Diameter 4	5.57	5.96	6.38

ANOVA						
	Cluster		Error		F	Sig.
	Mean Square	df	Mean Square	df		
Diameter 1	20.956	2	.087	359	239.969	.000
Diameter 2	22.550	2	.070	359	321.151	.000
Diameter 3	18.891	2	.054	359	349.591	.000
Diameter 4	14.926	2	.061	359	243.084	.000

Clustering Surgical Insertion (RW\_E16)

Final Cluster Centers			
	Cluster		
	shallow	average	deep
Surgical insertion	3.25	6.23	8.69

ANOVA						
	Cluster		Error		F	Sig.
	Mean Square	df	Mean Square	df		
Surgical insertion	561.926	2	.,845	359	665.328	.000



Clustering Electrode Position based on 16 Contact Distances (CD)

Final Cluster Centers		
	Cluster	
	Lateral	Medial
Contact Distance 16	2.24	1.97
Contact Distance 15	2.15	1.85
Contact Distance 14	2.11	1.74
Contact Distance 13	2.04	1.62
Contact Distance 12	1.97	1.50
Contact Distance 11	1.90	1.38
Contact Distance 10	1.79	1.25
Contact Distance 9	1.65	1.12
Contact Distance 8	1.48	.98
Contact Distance 7	1.28	.86
Contact Distance 6	1.08	.78
Contact Distance 5	.93	.74
Contact Distance 4	.83	.70
Contact Distance 3	.77	.65
Contact Distance 2	.75	.61
Contact Distance 1	.73	.58



ANOVA						
	Cluster		Error		F	Sig.
	Mean Square	df	Mean Square	df		
Contact Distance 16	6.214	1	.144	360	43.241	.000
Contact Distance 15	7.924	1	.100	360	79.632	.000
Contact Distance 14	11.790	1	.080	360	147.661	.000
Contact Distance 13	15.467	1	.065	360	238.353	.000
Contact Distance 12	19.484	1	.059	360	329.700	.000
Contact Distance 11	23.897	1	.054	360	439.101	.000
Contact Distance 10	25.836	1	.058	360	448.356	.000
Contact Distance 9	25.563	1	.060	360	427.840	.000
Contact Distance 8	21.657	1	.065	360	335.752	.000
Contact Distance 7	15.201	1	.068	360	222.106	.000
Contact Distance 6	8.208	1	.064	360	127.566	.000
Contact Distance 5	3.473	1	.073	360	47.506	.000
Contact Distance 4	1.588	1	.067	360	23.849	.000
Contact Distance 3	1.260	1	.058	360	21.641	.000
Contact Distance 2	1.713	1	.055	360	31.075	.000
Contact Distance 1	1.841	1	.052	360	35.622	.000



## APPENDIX B

## PCA Outcomes

## Principal Component Analysis

Principal Components Analysis (PCA) is a multivariate statistical technique developed to reduce the dimensionality of the data. This factor extraction method used to form uncorrelated linear combinations of the observed variables. The first component explains the largest amount of variance. Successive components explain progressively smaller portions of the variance and are all uncorrelated with each other. To calculate the PCA fits the factor scores are multiplied with the component matrix, and this is added to the average PCA score. The average PCA score defines the central pathway along the cochlear canal.

Component Matrix								
	Component							
	1	2	3	4	5	6	7	8
Radius 1	0.951	0.240	0.139	0.130	0.031	0.016	0.016	-0.001
Radius 2	0.966	0.206	-0.093	-0.076	0.055	0.040	-0.072	0.002
Radius 3	0.970	0.124	-0.177	-0.040	0.018	-0.056	0.080	0.016
Radius 4	0.973	-0.104	-0.173	0.051	-0.055	0.020	-0.007	-0.077
Radius 5	0.971	-0.189	-0.097	0.064	-0.022	-0.010	-0.037	0.078
Radius 6	0.960	-0.236	0.096	-0.040	0.066	0.073	0.048	0.001
Radius 7	0.974	-0.119	0.155	-0.022	0.041	-0.095	-0.035	-0.031
Radius 8	0.973	0.081	0.154	-0.065	-0.132	0.013	0.007	0.013

Average PCA scores for each radius	
	Average PCA Scores
Radius 1	4.524
Radius 2	3.433
Radius 3	3.066
Radius 4	2.567
Radius 5	2.352
Radius 6	1.992
Radius 7	1.730
Radius 8	1.525

